Chemical Science

ROYAL SOCIETY OF CHEMISTRY

EDGE ARTICLE

View Article Online
View Journal

Cite this: DOI: 10.1039/d6sc02299e

All publication charges for this article have been paid for by the Royal Society of Chemistry

De novo construction of C–O axial chirality *via* cobalt-catalyzed atroposelective C–H activation/annulation

Yanbo Zhang,†[a] Yichao Xie,†[a] Baicheng Guo,[a] Yingchao Dou,*[a] Dandan Yang*[a] and Jun-Long Niu*[ab]

Received 20th March 2026
Accepted 5th May 2026

DOI: 10.1039/d6sc02299e

rsc.li/chemical-science

The catalytic asymmetric synthesis of axially chiral compounds has attracted growing attention over the past decades. C–O axially chiral compounds represent a distinctive class of atropisomers characterized by a unique dual-axial architecture. Their atroposelective construction remains a formidable challenge due to inherent low rotational barriers and high conformational flexibility. Current catalytic approaches rely predominantly on enantioselective desymmetrization of preformed diaryl ethers. Here, we report an unprecedented *de novo* synthetic strategy, enabling the construction of a new class of C–O axially chiral aryl-heterocyclic ethers. This protocol is achieved by an earth-abundant cobalt-catalyzed atroposelective C–H activation/annulation of arylamides with phenylethynyl ethers, which concurrently builds the heterocycle and the C–O chiral axis in a single step. Notably, a traceless directing group strategy is successfully implemented, featuring smooth *in situ* cleavage. Furthermore, a series of C–O atropisomers bearing multiple stereogenic elements are prepared with excellent stereoselectivity. Racemization experiments reveal high configurational stability of the products. Derivatization studies afford a versatile library of non-biaryl C–O axially chiral scaffolds, extending the applicability of this strategy.

Introduction

Developing efficient strategies for the construction of diverse chiral entities has long been a central pursuit in chemical research.[1–10] In contrast to the extensively studied point chirality, axial chirality arises from restricted rotation around a stereogenic axis. Given the widespread application of atropisomeric frameworks in pharmaceuticals and advanced materials, substantial efforts have been devoted to their asymmetric construction. Distinct from well-established mono-axial chiral systems (Fig. 1a), such as C–C, C–N, C–B, and N–N atropisomers, the distinctive C–O axially chiral architecture features a unique dual-axial chirality,[11–15] wherein two contiguous C–O axes are bonded to a central oxygen atom. This structural motif is not only prevalent in bioactive molecules and natural products,[16–23] but also serves as a privileged scaffold in functional molecules[24] and phosphine ligands[25–28] (Fig. 1b). Despite their significance, the asymmetric construction of C–O atropisomers remains largely underdeveloped, and is hindered by several intrinsic challenges: (1) the inherently low rotational barriers associated with two contiguous C–O axes endow C–O axially chiral compounds with flexible atropisomerism,[29] triggering facile racemization *via* concerted rotation of both axes; (2) simultaneous stereocontrol over two C–O axes complicates the achievement of high atroposelectivity compared to mono-axial chirality molecules; (3) the oxygen bridge between the two C–O axes weakens spatial and electronic interactions of substituents, resulting in enhanced conformational freedom. Consequently, these factors collectively compromise the configurational stability and synthetic accessibility of dual-axial scaffolds, making their catalytic asymmetric synthesis a considerable challenge.

Since the pioneering investigations of C–O atropisomers by Fuji,[30] the catalytic asymmetric construction of such architectures has gained growing attention in the synthetic community and represents a significant frontier in modern stereochemistry.[11–15,31,32] Several elegant catalytic enantioselective approaches toward C–O atropisomers have been achieved (Fig. 1c). However, current strategies rely mostly on atroposelective desymmetrization *via* enzymatic,[33,34] organocatalytic[35–43] or transition-metal-catalyzed functionalizations,[44–48] and focus predominantly on the synthesis of C–O axially chiral diaryl ether frameworks. The exclusive construction of axially chiral naphthoquinone-aryl ethers was achieved by Gustafson *via* a dynamic kinetic resolution approach.[49] Given the significance of privileged C–O axial structures, it is highly desirable to develop novel synthetic strategies that could enable the efficient

[a]*College of Chemistry, Pingyuan Laboratory, Zhengzhou University, Zhengzhou, 450001, China. E-mail: yingchaodou@zzu.edu.cn; yangdandan@zzu.edu.cn; niujunlong@zzu.edu.cn*

[b]*State Key Laboratory of Coking Coal Resources Green Exploitation, Zhengzhou University, Zhengzhou, 450001, China*

† These authors contributed equally to this work.

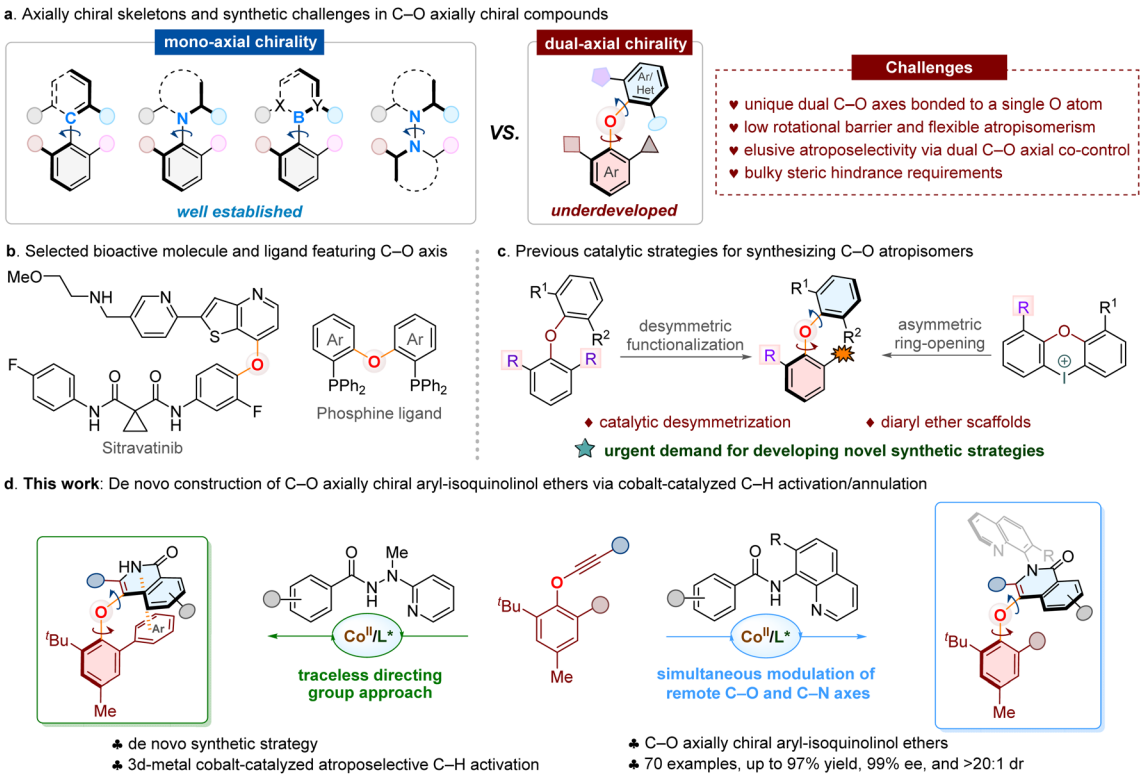

Fig. 1 Background and project synopsis for the synthesis of C–O atropisomers. (a) Axially chiral skeletons and synthetic challenges in C–O axially chiral compounds. (b) Selected bioactive molecule and ligand featuring C–O axis. (c) Previous catalytic strategies for synthesizing C–O atropisomers. (d) This work: *de novo* construction of C–O axially chiral aryl-isoquinolinol ethers *via* cobalt-catalyzed C–H activation/annulation.

construction of C–O atropisomers with broader structural diversity.

Over the past decades, the transition-metal catalyzed[50–53] asymmetric C–H activation has emerged as an atom-economical and versatile platform for accessing enantiopure molecules. However, forging C–O axially chiral compounds *via* this versatile approach has not been realized to date. More recently, the 3d-metal cobalt-catalyzed asymmetric C–H activation[53–58] has attracted considerable attention since the independent establishment of cobalt/salicyloxazoline (Salox) catalytic system by the Shi group[59] and our group.[60] This 3d-metal platform has enabled facile access to diverse axially chiral architectures, including C–C, C–N, and N–N atropisomers.[60–79] Inspired by these achievements, we hypothesized that the cobalt/Salox catalysis could offer a promising solution for synthesizing C–O atropisomers.

Herein, we report an unprecedented *de novo* synthetic strategy, delivering a new type of C–O axially chiral aryl-heterocyclic ethers that differ from the previously reported diaryl ether compounds (Fig. 1d). This protocol is successfully implemented through a cobalt-catalyzed atroposelective C–H activation/annulation of benzamides with rationally designed phenylethynyl ethers. The simultaneous construction of both the isoquinolinone heterocycle and the C–O chiral axis is faciliated in a single synthetic step. Notably, a traceless directing group approach is achieved using 2-(1-methylhydrazinyl)pyridine, which is cleaved *in situ* during the reaction. Meanwhile, a diverse array of C–O axially chiral compounds bearing multiple stereogenic elements are obtained with high stereoselectivity *via* the smoothly synchronous modulation of remote C–O and C–N axes. Moreover, high configurational stability is identified for the prepared C–O atropisomers through racemization studies. X-ray crystallography reveals a non-covalent π–π interaction between the isoquinolinone ring and the phenyl substituent of the phenylethynyl ether, likely contributing to both stereocontrol and the configurational stabilization of obtained products.

Results and discussion

Optimizing reaction conditions

We began the investigations by subjecting phenylethynyl ether **1a** and benzamide **2a** preinstalled with 2-(1-methylhydrazinyl) pyridine[74,80–83] as directing group to the cooperative Co/Salox catalytic system. Initially, various chiral Salox ligands were evaluated in combination with $Co(OAc)_2 \cdot 4H_2O$ as catalyst, $Mn(OAc)_2 \cdot 4H_2O$ as oxidant in 2-BuOH (0.1 M) at 60 °C for 10 h under air atmosphere (Table 1). Gratifyingly, the desired product **3a** could be obtained in 91% yield with 75% ee in the presence of **L1**, and the directing group could be removed *in situ* during the transformation. Then the steric and electronic influence of substituents on the ligand were examined. The *ortho*-substituted **L2**, **L3** and **L4** afforded **3a** with improved enantioselectivities (85%, 95%, and 90% ee, respectively), and the yields remained low (56%, 17%, and 23%, respectively). Introducing *para*-

Table 1 Optimization studies

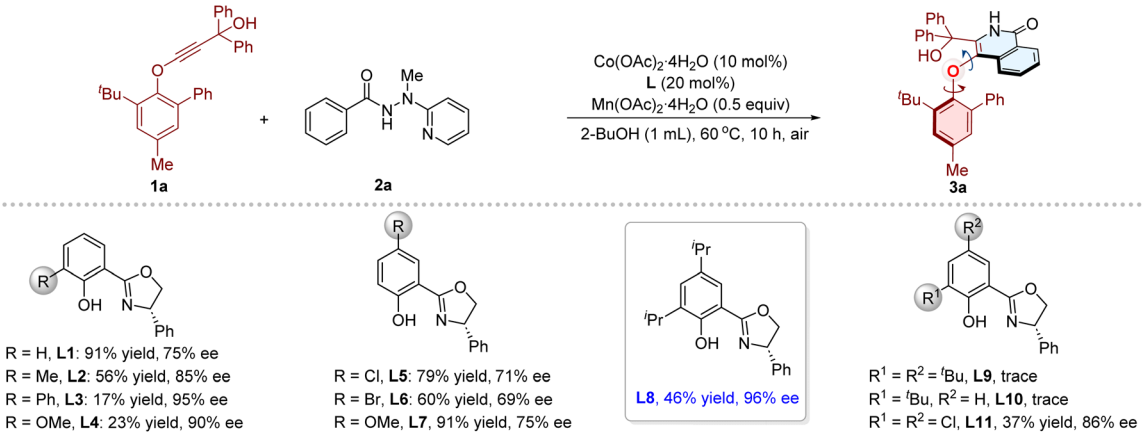

Entry[a]	[Co]	[Mn] (*x* equiv.)	Solvent	*T* (°C)	*t* (h)	Yield (%)	ee (%)
1	$Co(OAc)_2 \cdot 4H_2O$	0.5	2-BuOH	60	10	46	96
2	$CoSO_4 \cdot 7H_2O$	0.5	2-BuOH	60	10	Trace	—
3	$CoBr_2$	0.5	2-BuOH	60	10	18	95
4	$Co(acac)_2$	0.5	2-BuOH	60	10	Trace	—
5	$Co(OAc)_2 \cdot 4H_2O$	0.7	2-BuOH	60	10	43	96
6	$Co(OAc)_2 \cdot 4H_2O$	0.3	2-BuOH	60	10	39	96
7	$Co(OAc)_2 \cdot 4H_2O$	0.5	*t*-BuOH	60	10	45	96
8	$Co(OAc)_2 \cdot 4H_2O$	0.5	*n*-BuOH	60	10	24	89
9	$Co(OAc)_2 \cdot 4H_2O$	0.5	*n*-PrOH	60	10	17	93
10	$Co(OAc)_2 \cdot 4H_2O$	0.5	EtOH	60	10	21	94
11	$Co(OAc)_2 \cdot 4H_2O$	0.5	2-BuOH	80	10	46	94
12	$Co(OAc)_2 \cdot 4H_2O$	0.5	2-BuOH	100	10	43	92
13	$Co(OAc)_2 \cdot 4H_2O$	0.5	2-BuOH	60	20	63	96
14	$Co(OAc)_2 \cdot 4H_2O$	0.5	2-BuOH	60	30	78	96
15	$Co(OAc)_2 \cdot 4H_2O$	0.5	2-BuOH	60	36	89	96

[a] Reaction conditions: **1a** (0.12 mmol), **2a** (0.1 mmol), cobalt catalyst (10 mol%), ligand (20 mol%), $Mn(OAc)_2 \cdot 4H_2O$ (*x* equiv.), solvent (1 mL), *T*/°C, *t*/h, air, isolated yields, the ee values were determined by HPLC analysis.

substituents (**L5**, **L6**, **L7**) had negligible effect on the stereoselectivity of this reaction. Notably, a superior result was obtained in the presence of **L8**, which features *ortho*- and *para*-isopropyl substituted phenol moiety, delivering **3a** in 46% yield with 96% ee. The more sterically bulky **L9** and **L10** gave only trace amount of product. Subsequently, other reaction parameters, including cobalt salts, solvents, reaction temperature, and dosages of cobalt, ligand, and oxidants, were systematically optimized (Table 1 and S1–S9 in the SI). The best performance was attained under the conditions as shown in entry 15: $Co(OAc)_2 \cdot 4H_2O$ (10 mol%) as catalyst, **L8** (20 mol%) as ligand, $Mn(OAc)_2 \cdot 4H_2O$ (0.5 equiv.) as co-oxidant, in 2-BuOH at 60 °C under air atmosphere, and the desired product **3a** was obtained in 89% yield with 96% ee. Moreover, the use of other directing groups, such as 2-(1-ethylhydrazinyl)pyridine, 2-(1-propylhydrazinyl)pyridine, and 2-(1-benzylhydrazinyl)pyridine (Table S10), also afforded product **3a** (81%, 96% ee; 77%, 96% ee; 18%, 96% ee, respectively).

Reaction substrate scope

After establishing the optimal reaction conditions, we proceeded to evaluate the generality of this cobalt/Salox-catalyzed atroposelective synthesis of C–O axially chiral compounds. First, the substrate scope of benzamides was examined (Fig. 2). Substrates bearing diverse functionalities, including *para*-fluoro, chloro, bromo, iodo, methyl, *tert*-butyl, phenyl, methoxyl, trifluoromethoxy, and nitrile groups, reacted smoothly with phenylethynyl ether **1a**, delivering the corresponding C–O axially chiral products (**3b–3k**) in good yields (69–95%) with excellent enantioselectivities (94–99% ee). The benzamides featuring *para*-sterically bulky anthracene or carbazole substituents were also able to give products **3l** and **3m** (54% yield, 65% ee, and 85% yield, 85% ee, respectively). Compound **3n** was obtained as the sole product in 85% yield with 96% ee starting from *meta*-methyl substituted benzamide. The *ortho*-methyl substituted substrate reacted to deliver **3o** in 35% yield with 95% ee. The substrates with extended aromatic systems, including either naphthalene or pyrene, were smoothly transformed into corresponding products **3p** and **3q** in 18% yield with 95% ee, and 71% yield with 94% ee, respectively.

Subsequently, the compatibility of phenylethynyl ethers was investigated with benzamide **2a** under the optimized conditions (Fig. 3). The alkynes bearing divergent substituted aryl on the

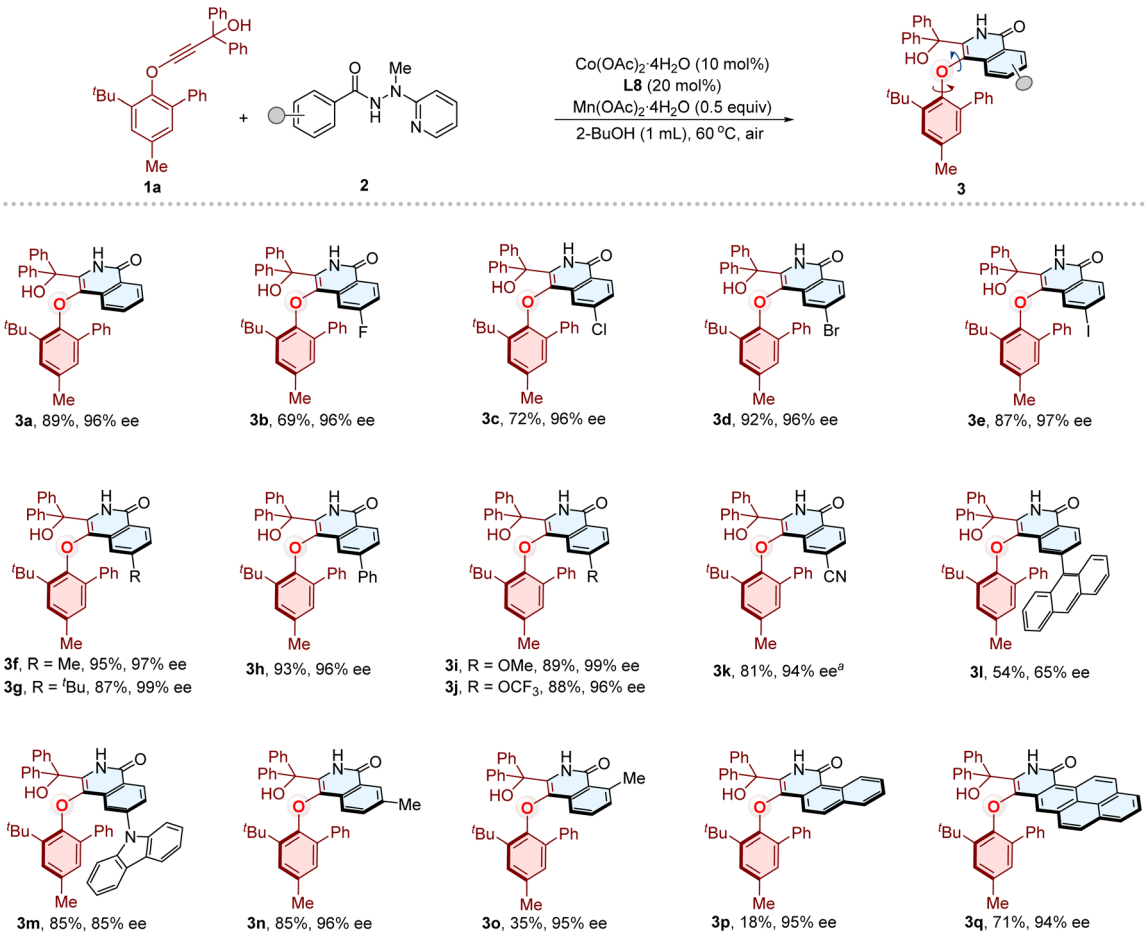

Fig. 2 Scope of benzamides for the synthesis of C–O axially chiral aryl-isoquinolinol ethers. Reaction conditions: **1a** (0.12 mmol), **2** (0.1 mmol), $Co(OAc)_2 \cdot 4H_2O$ (10 mol%), **L8** (20 mol%), $Mn(OAc)_2 \cdot 4H_2O$ (0.5 equiv.), 2-BuOH (1 mL), 60 °C, 36 h, air, isolated yields, the ee values were determined by HPLC analysis. [a]48 h.

phenolic motif, including *para*-halogen, alkyl, and aryl substituted phenyl substituents, were well tolerated, furnishing the corresponding C–O axially chiral compounds (**3r–3v**) in 85–96% yield with 94–97% ee values. The strong electron-withdrawing CF_3 group did not interfere with the reaction, giving **3w** in 92% yield with 95% ee. The *meta*-alkyl substituted substrate also reacted well to afford **3x** (80% yield, 96% ee). We then examined modifications on the *gem*-diaryl propargyl alcohol motif. The products (**3y–3z**, **3za–3zf**) bearing *para*-halogen, electron-donating, electron-withdrawing groups and *meta*-chloro groups on the *gem*-diaryl motif were produced smoothly in 83–97% yields with 96–97% ee values. The absolute configuration of **3za** was confirmed by X-ray crystallographic diffraction (Fig. 3, **3za**, CCDC 2516693), and detailed analysis indicates a typical π–π interaction (typical π-stacking distances, face to face separations, 3.4–3.8 Å,[84] find details in the SI, Fig. S8) between the isoquinolinone ring and the phenyl substituent of arylether moiety. This weak interaction might play a key role in the stereocontrol of the transformation, meanwhile potentially contribute to the configurational stability of C–O axially chiral products. The fluorene and thiophene derived alkynes were also suitable, affording **3zg** and **3zh** in 55% yield with 85% ee, and 81% yield with 80% ee, respectively. To evaluate steric effects of the tertiary propargyl alcohol motif, we replaced *gem*-diaryl group with less hindered alternatives. Using a *gem*-dimethyl, cyclopentyl- and cyclohexyl-substituted substrates furnished corresponding products **3zi–3zk** in 73–95% yields with moderate enantioselectivities (77–81% ee values). Compound **3zl** was obtained in 90% yield with only 27% ee. The low enantioselectivity likely arises from the loss of π–π interaction upon replacement of the phenyl group by a methyl group, which would reduce the rotational barrier. The alkynes containing unsymmetrical tertiary alcohol motif was also examined, furnishing products **3zm** ($\Delta G^{\ddagger}$ = 31.9 kcal mol^{-1}, Table S19 and Fig. S4–S5) in 87% yield (8 : 1 dr, 83% ee). Afterwards, we examined the scope of nonpropargyl substrates. Notably, the phenylethynyl ether bearing a TMS group in place of the tertiary alcohol motif provided both desired product **3zn** (35%, 82% ee) and compound **3zn′** (21%, single diastereomer, 99% ee). The latter, with directing group still attached, possesses multiple chiral elements involving remote C–O and C–N axial chiralities.

In recent years, the enantioselective construction of molecules containing multiple axially chiral elements has garnered

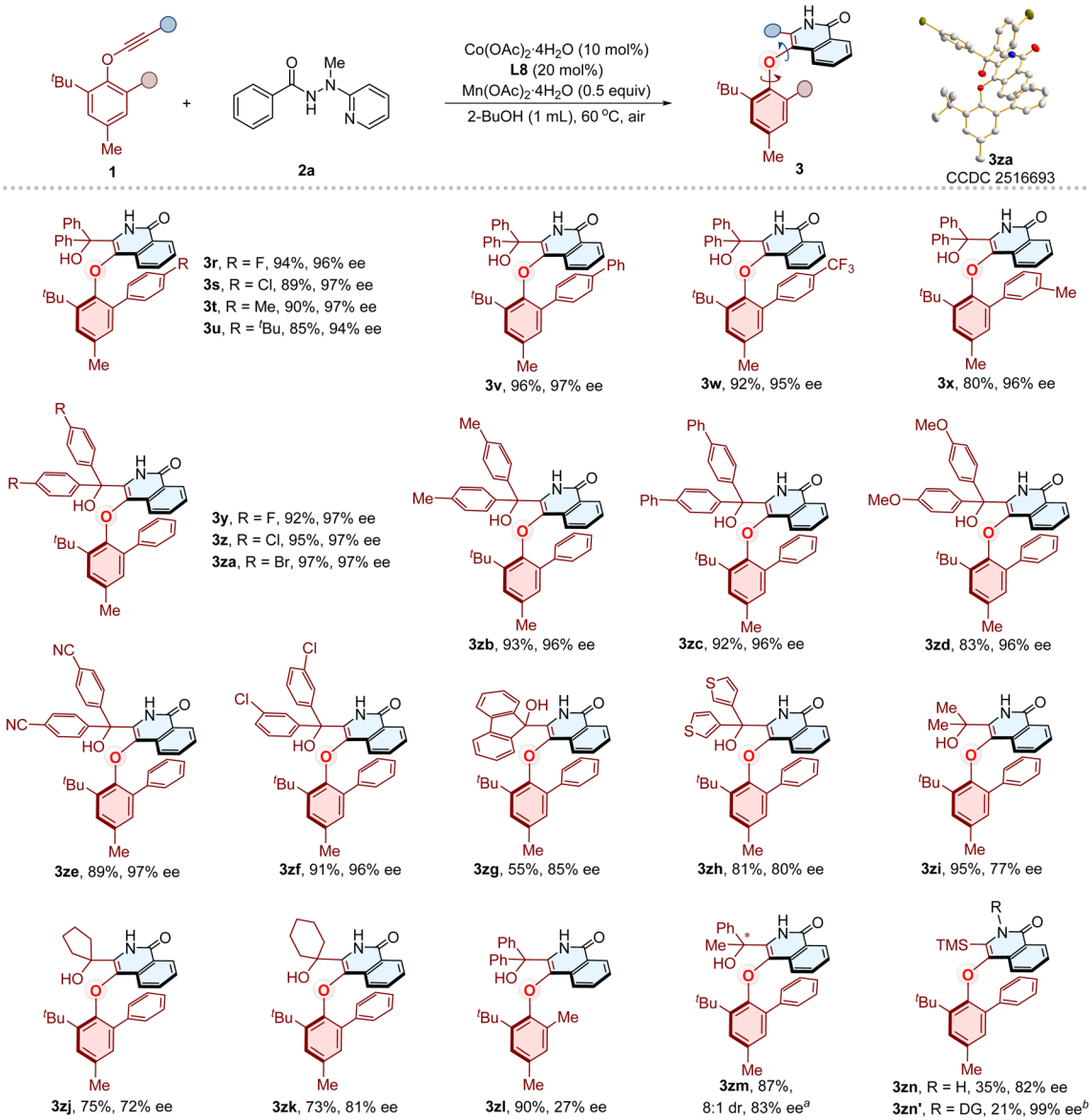

Fig. 3 Scope of phenylethynyl ethers for the synthesis of C–O axially chiral aryl-isoquinolinol ethers. Reaction conditions: **1** (0.12 mmol), **2a** (0.1 mmol), $Co(OAc)_2 \cdot 4H_2O$ (10 mol%), **L8** (20 mol%), $Mn(OAc)_2 \cdot 4H_2O$ (0.5 equiv.), 2-BuOH (1 mL), 60 °C, 36 h, air, isolated yields, the ee values were determined by HPLC analysis. [a]The dr value was determined by ^{1}H-NMR. [b]Compound **3zn'** was obtained as single diastereomer, DG = 2-(methylamino)pyridine.

increasing attention from the synthetic community.[9,61,69,72–77,85–99] However, the synthesis of such architectures featuring C–O axial chirality has not been achieved. Accordingly, we sought to explore the simultaneous installation of both C–O and C–N chiral axes under the aforementioned conditions.

Initially, the synthesis of compound **5a** from phenylethynyl ether **1x** and benzamide **4a** bearing 8-aminoquinoline as directing group was set as a template to verify this concept. Gratifyingly, further optimization of this reaction (based on the previously established conditions, Table S11–S14 in SI) provided satisfactory results. Under the optimized conditions, the desired product **5a** was obtained in 89% yield, 19 : 1 dr and 99% ee with $Co(OAc)_2 \cdot 4H_2O$ (10 mol%) as catalyst, **L8** as ligand, $Mn(OAc)_2 \cdot 4H_2O/O_2$ as the oxidant, NaOPiv·H_2O (1 equiv.) as the additive, in 2-BuOH (0.1 M) at 40 °C under air atmosphere. The absolute configuration of **5a** was confirmed by X-ray crystallographic diffraction (Fig. 4, **5a**, CCDC 2504636). The π–π interaction (find details in the SI, Fig. S9) between the isoquinolinone ring and the phenyl substiuent of phenolic moiety was also observed, which might be helpful for the stabilization of the configuration. Then the generality of this approach was scrutinized under the optimal conditions (Fig. 4). Benzamides substituted with *para*-halogen (including F, Cl, Br, I), or alkyl groups (Me, ^{t}Bu) were all accommodated to give corresponding products (**5b–5g**) in 82–92% yield with 12:1–16 : 1 dr and 96–99% ee. Substrates with either electron-donating (OMe) or electron-withdrawing (OCF_3, CN, CF_3) groups at the *para* position were well tolerated, furnishing products **5h–5k** in 90–96%

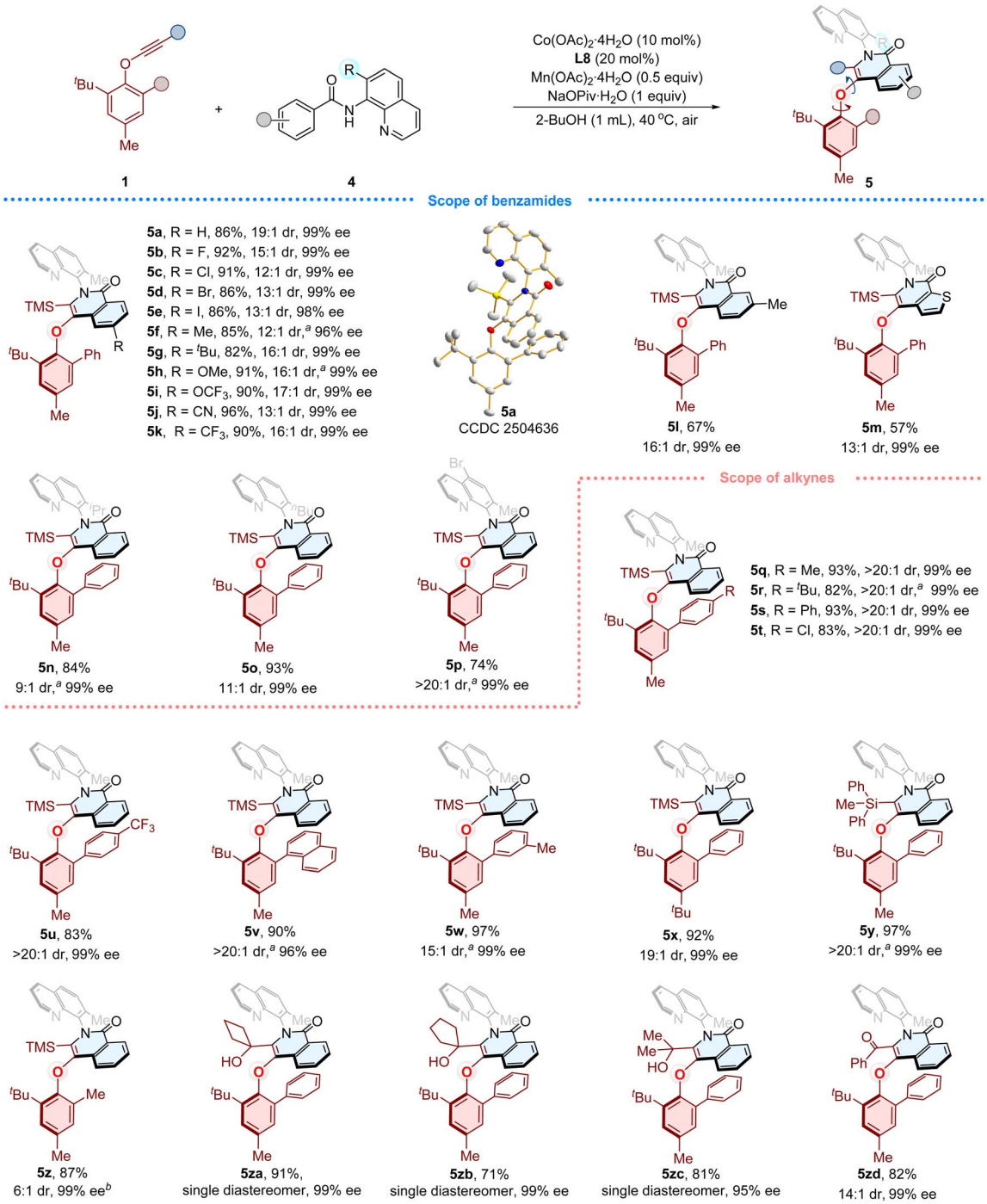

Fig. 4 Substrate cope for the synthesis of C–O/C–N diaxially chiral compounds. Reaction conditions: **1** (0.12 mmol), **4** (0.1 mmol), $Co(OAc)_2 \cdot 4H_2O$ (10 mol%), **L8** (20 mol%), $Mn(OAc)_2 \cdot 4H_2O$ (0.5 equiv.), $NaOPiv \cdot H_2O$ (1 equiv.), 2-BuOH (1 mL), 40 °C, 36 h, air, the dr values were determined by HPLC analysis. [a]The dr value was determined by ^{1}H-NMR. [b]Ligand **L9** was used instead of **L8**.

yields with 13:1–17 : 1 dr and 99% ee. The *meta*-methyl-substituted benzamide provided **5l** in 67% yield (16 : 1 dr, 99% ee). Compound **5m** was obtained in 57% yield with 13 : 1 dr and 99% ee arising from 2-thiophenecarboxamide derivative. Afterwards, replacing the methyl with bulky isopropyl and tertiary butyl groups at 8-aminoquinoline furnished corresponding products **5n** and **5o** in good yields (84%, 93%, respectively) with 99% ee and moderate diastereoselectivity (9 : 1, 11 : 1 dr). Notably, the substrate with 5- bromo-substituted directing group afforded **5p** in 74% yield with excellent diastereoselectivity (>20 : 1 dr, 99% ee). The compatibility of diverse phenylethynyl ethers was then evaluated. The alkynes bearing *para*-methyl, *tert*-butyl, phenyl, chloro, and CF_3 substituted phenyl groups on the phenolic motif were well

tolerated to give products (**5q–5u**) in 82–93% yield with >20 : 1 dr and 99% ee. The naphthyl-containing alkynes gave **5v** in 90% yield (>20 : 1 dr, 96% ee). The *meta*-methyl substituted substrate afforded **5w** in 97% yield (15 : 1 dr, 99% ee). The substrate with *para*-^{t}Bu in place of methyl at phenol moiety remained efficient, providing **5x** in 92% yield (19 : 1 dr, 99% ee). Introducing a more bulky Ph_2MeSi group instead of TMS smoothly afforded **5y** in 97% yield (>20 : 1 dr and 99% ee). Replacing the phenyl with methyl afforded **5z** in 87% yield with 6 : 1 dr and 99% ee. We also examined modifications of phenylethynyl ether by installing tertiary alcohol motif in place of TMS group. The compounds **5za–5zc** were successfully obtained in good yields (71–91%) with excellent stereocontrol (single diastereomer, 95–99% ee). Finally, replacing the TMS group with a benzoyl group provided compound **5zd** in 82% yield with 14 : 1 dr and 99% ee.

Further transformations and synthetic applications

To demonstrate the synthetic utility of this protocol, gram-scale preparations of the representative C–O axially chiral compounds were carried out. Compound **3a** was prepared in a reaction scale of 2.5 mmol, affording a good result without erosion on reaction efficacy and stereoselectivity (1.20 g, 83% yield, 96% ee) (Fig. 5a). Furthermore, a series of downstream transformations were performed on product **3a**. The free N–H

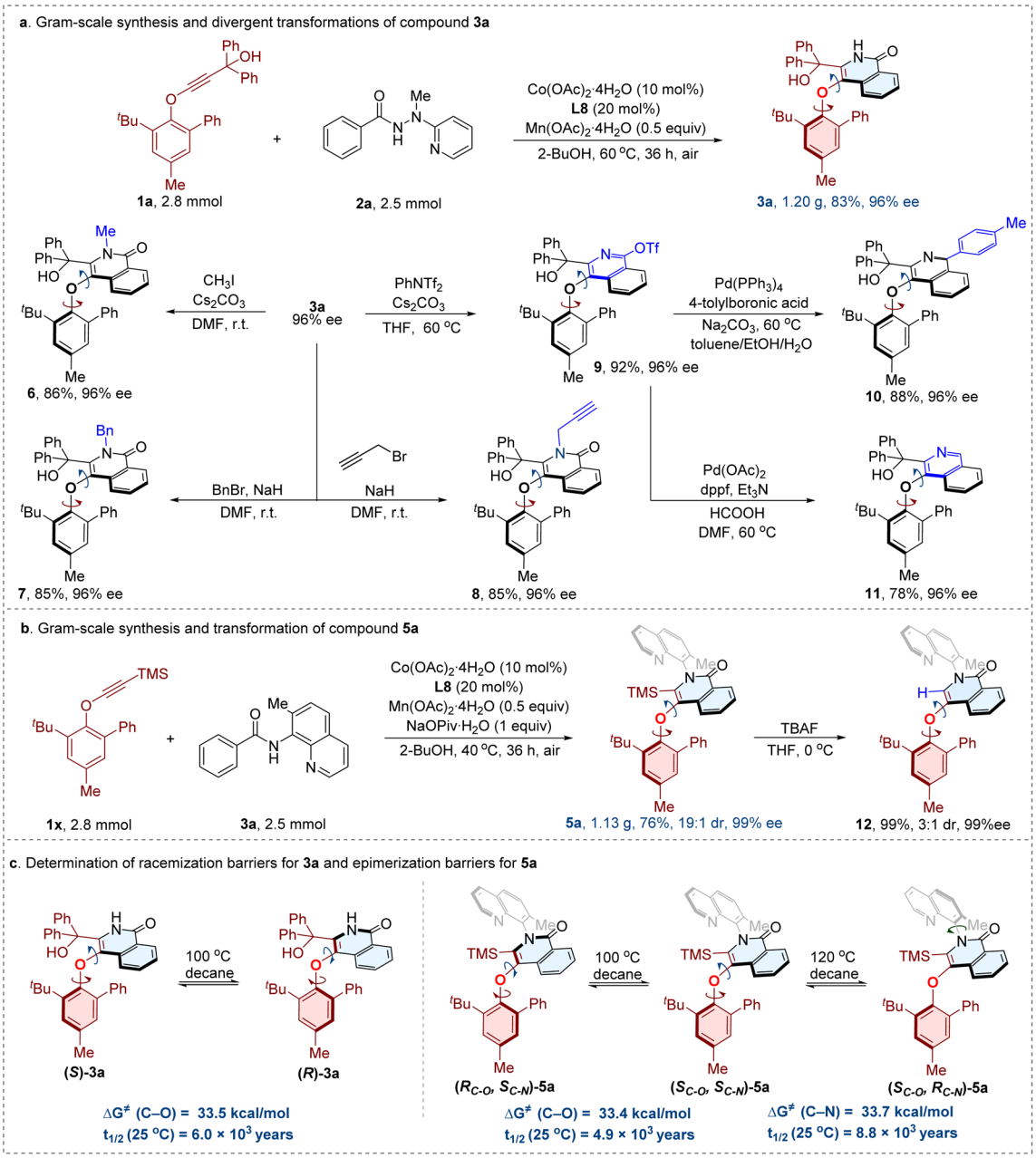

Fig. 5 Investigations of synthetic utilities. (a) Gram-scale synthesis and divergent transformations of compound **3a**. (b) Gram-scale synthesis and transformation of compound **5a**. (c) Determination of racemization barriers for **3a** and epimerization barriers for **5a**.

moiety of the isoquinolinone core could be readily functionalized: alkylations with methyl iodide, benzyl bromide, or propargyl bromide furnished products **6**, **7**, and **8** in good yields (86%, 85%, and 85%, respectively) without loss of enantiopurity. Additionally, treatment of **3a** with $PhNTf_2$ and Cs_2CO_3 in THF at 60 °C provided the C–O axially chiral aryl-isoquinoline ether compound **9** in 92% yield with 96% ee. This intermediate served as a versatile precursor for further diversifications. For instance, a $Pd(PPh_3)_4$-catalyzed Suzuki–Miyaura cross-coupling reaction with 4-tolylboronic acid delivered compound **10** in 88% yield with 96% ee. Subsequent removal of OTf group under $Pd(OAc)_2$/dppf catalysis afforded compound **11** in 78% yield with 96% ee. Throughout all derivatizations, no erosion of enantiomeric purity was observed, underscoring the robustness of the chiral framework under diverse reaction conditions. The gram-scale synthesis of compound **5a** maintained excellent stereoselectivity (19 : 1 dr, 99% ee), and only slight decreased yield (76%) was observed (Fig. 5b). Finally, desilylation of **5a** with TBAF smoothly gave compound **12** in 99% yield with 3 : 1 dr and 99% ee. The results indicates that removal of TMS group decreases the rotational energy barrier of C–O axis, while with negligible effect on the stability of C–N axis. Furthermore, the experimental studies of racemization barriers (Fig. 5c) for compound **3a** (recovery: 90%) afforded a $\Delta G^{\ddagger}$ (C–O) value of 33.5 kcal mol^{-1}, with a half-time ($t_{1/2}$) of 6.0×10^3 years at 25 °C. The measurement of epimerization barriers for compound **5a** (recovery: 91%, 100 °C; 89%, 120 °C) revealed a $\Delta G^{\ddagger}$ (C–O) value of 33.4 kcal mol^{-1}, and a $\Delta G^{\ddagger}$ (C–N) value of 33.7 kcal mol^{-1}. The half-times ($t_{1/2}$) were determined to be 4.9 $\times 10^3$ years for C–O axis and 8.8×10^3 years for C–N axis at 25 °C, respectively. These detailed studies underscore the high stability of prepared C–O axially chiral scaffolds.

Afterwards, the ultraviolet-visible spectroscopy and fluorescence spectrum (Table S21–23) of representative C–O atropisomers were studied. The substitution patterns at either the benzamide or alkyne moieties had negligible effect on the maximum absorption wavelength in UV-vis of compounds **3** and **5**. Among the C–O axially chiral products **3** and **5**, introducing *para*-bromo (**3d**), iodo (**3e**), cyano (**3k**), and *ortho*-alkyl (**3o**) groups at the isoquinolinone moiety resulted in blue shift for the fluorescence spectrum, as well as compound 3zh with *gem*-dithiophene tertiary alcohol motif. Pronounced red shift was observed for compounds with *para*-phenyl (**3h**), carbazole (**3m**) group or extended aromatic fragments (**3p**, naphthalene, and **3q**, pyrene, respectively). Compound **5a** (446 nm) bearing diaxial architecture displayed a bathochromic shift compared with **3a** (410 nm). Introducing *para*-^{t}Bu (**5g**), methoxy (**5h**), and cyano (**5j**) led to evident red shift. The longest maximum emission wavelength (540 nm) was obained with compound **5v** bearing a naphthyl group at the phenol moiety. In comparison,

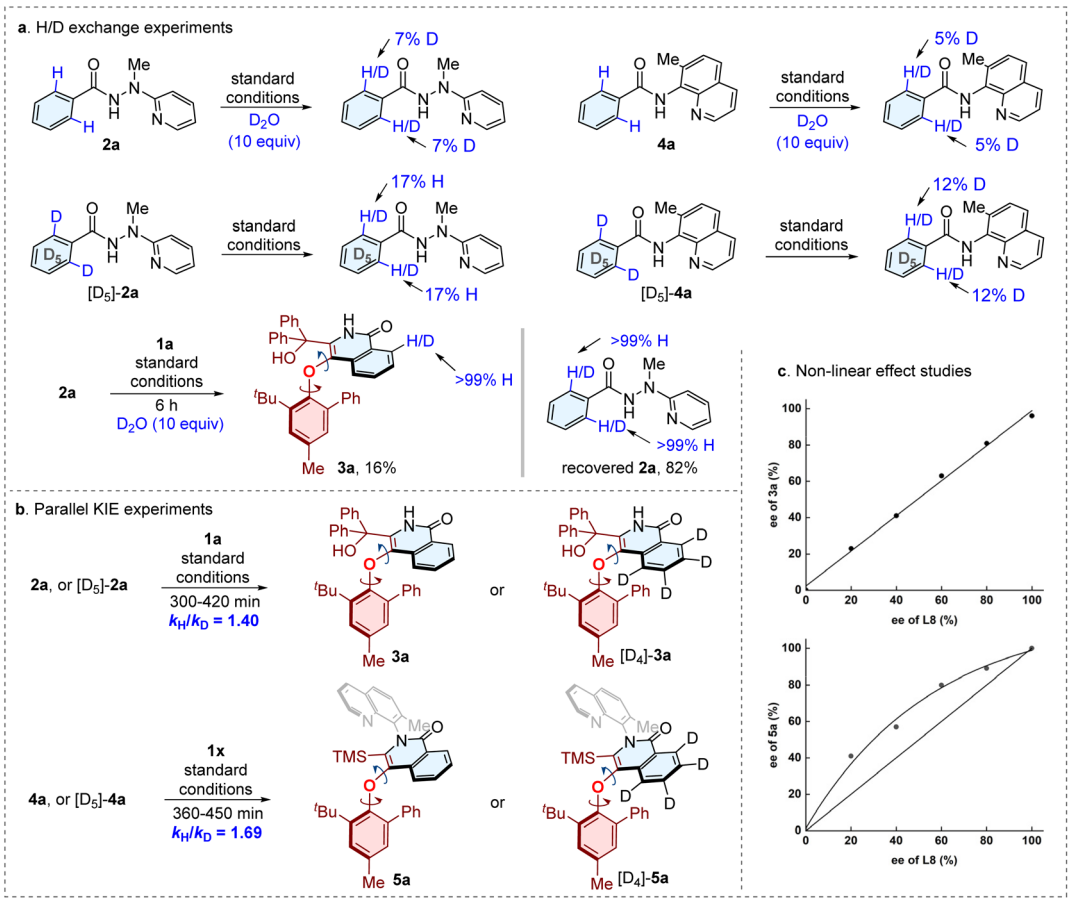

Fig. 6 Mechanistic studies. (a) H/D exchange experiments. (b) Parallel KIE experiments. (c) Non-linear effect studies.

compound **5zd** with a benzoyl group instead of TMS exhibits the shortest maximum emission wavelength (414 nm). Notably, a dual emission was observed for compounds **3h**, **3p**, **3q**, and **5w** at 375 nm and 444 nm, 370 nm and 445 nm, 388 nm and 518 nm, 394 nm and 502 nm, respectively (Fig. S10).

Mechanistic studies

To gain insights into this transformation, several deuterium-labeling experiments were conducted (Fig. 6). The H/D exchange experiments (Fig. 6a) were carried out with **2a** or [D_5]-**2a**, as well as **4a** or [D_5]-**4a** in the absence of alkynes, detecting measurable H/D exchangement. The outcomes demonstrate that the C–H cleavage step is reversible. Meanwhile, we performed the H/D exchange experiments of **2a** with **1a** under standard conditions for 6 h, and no deuteration was observed. These findings are consistent with a reversible C–H activation, with the subsequent alkyne insertion being considerably faster. Subsequently, two sets of parallel (Fig. 6b) kinetic isotope effects (KIE) studies at low conversions gave k_H/k_D values of 1.40 and 1.69, respectively. The results suggest that C–H bond activation is likely not involved in the rate-determining step. Moreover, the non-linear effect (NLE) studies for the traceless directing group approach revealed a linear relationship between the ee values of chiral Salox ligand and the C–O axially chiral product **3a**. However, a positive NLE outcomes was obtained for the synthesis of C–O/C–N diaxially chiral compound **5a**, which indicates that multiple chiral ligands perhaps participate in the coordination to form the cobalt species in the catalytic cycle.

Based on the experimental results and literature reports,[53–55] we proposed a plausible mechanism as shown in Fig. 7. In the presence of chiral ligand **L8**, the Co(II) is oxidized by O_2/$Mn(OAc)_2\cdot 4H_2O$ to form active Co(III) species **Int-1**. In the case with 7-methyl-8-aminoquinoline as the directing group, a positive NLE result indicates that two ligands might coordinates with Co to form complex $[Co\text{-}L_2]_n$ species **Int-1′**.[100] The **Int-1** or **Int-1′** undergoes coordination with benzamides **2a** or **4a** bearing different directing groups, and C–H activation to afford **Int-2** and **Int-2′**, respectively. The following ligand exchange and migration insertion of **Int-2** with alkyne **1a** delivers a seven-membered alkenyl cobaltacycle intermediate **Int-3**. The subsequent reductive elimination provides a Co(I) species **Int-4**, which is likely to be stabilized by two non-covalent π–π interactions. The first interaction arises between the phenyl moiety of the oxazoline scaffold and the pyridyl unit of the directing group. The second one is established between the isoquinolinone ring and the phenyl

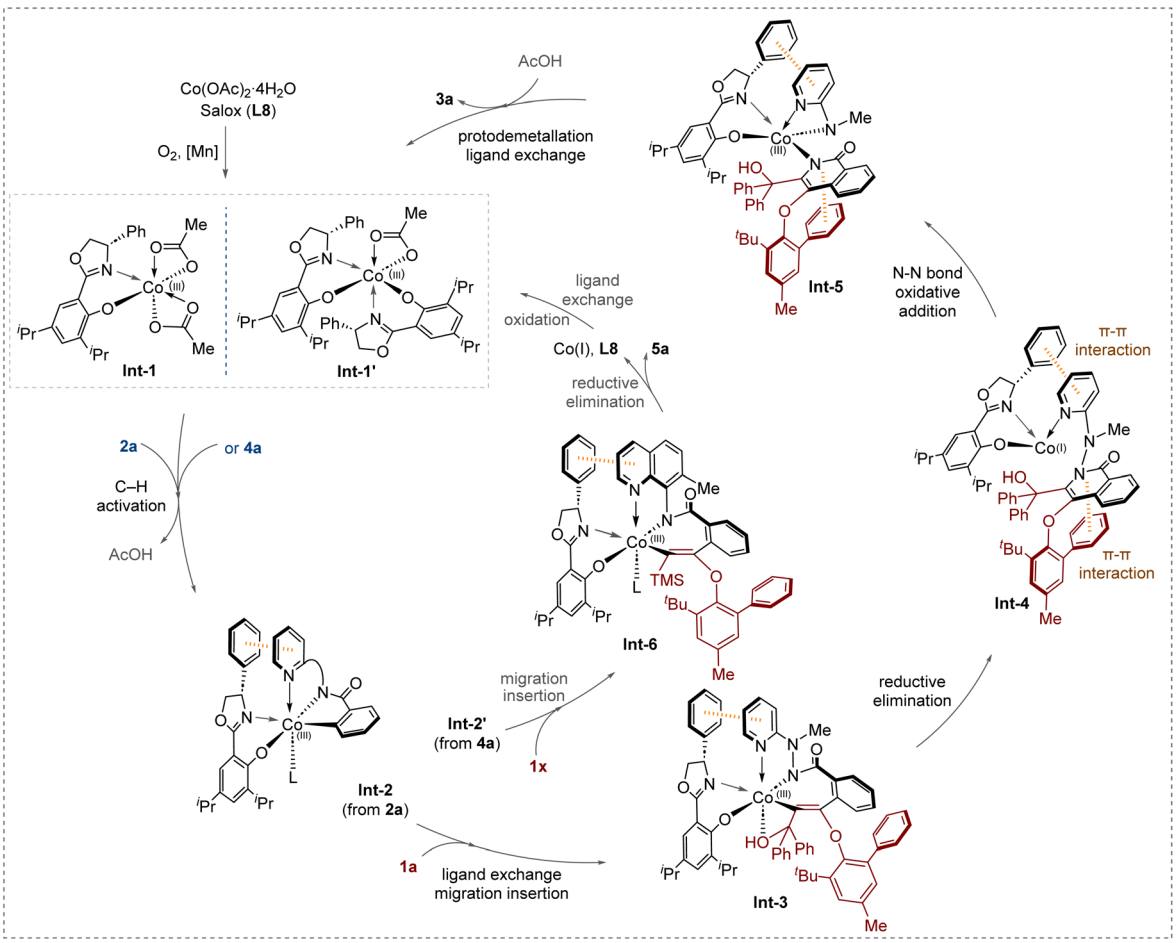

Fig. 7 Proposed mechanism.

substituent of the phenylethynyl ether. The latter is corroborated by X-ray crystallographic diffraction data for compounds **3za** and **5a** (Find details in Table S8–S9 in SI). Collectively, these two π–π stacking interactions are postulated to play a pivotal role in stabilizing the cobalt species and the axial chirality configuration of the products. The **Int-4** is transformed to Co(III) **Int-5** *via* an oxidative addition of Co(I) to N–N bond.[80–83,101] Finally, protodemetallation and ligand exchange of **Int-5** affords the desired C–O axially chiral aryl-isoquinolinone ether **3a**, and simultaneously releases the Co(III) catalyst and **L8**. In the case of benzamide **4a** bearing 7-methyl-8-aminoquinoline as the directing group, the corresponding intermediate **Int-2′** undergoes migration insertion with alkyne **1x** to give **Int-6**. After the subsequent reductive elimination, the final C–O/C–N diaxially chiral product **5a** was produced. The regenerated Co(I) could be further oxidized to active Co(III) species.

Conclusions

In conclusion, we have developed an atroposelective construction of a new type of C–O axially chiral aryl-heterocyclic ethers through Co/Salox catalyzed asymmetric C–H activation/annulation of benzamides with phenylethynyl ethers. This strategy features a *de novo* synthetic approach, enabling simultaneous establishments of heteroaromatic ring and C–O chiral axis. A broad range of C–O axially chiral aryl-isoquinolinol ethers were efficiently synthesized with excellent stereoselectivity. Notably, the achievement of *in situ* removal of *N*,*N*-bidentate directing group secured the traceless directing approach. Moreover, an array of structurally diverse C–O axially chiral products bearing multiple chiral axes were afforded in good yields, accompanied by excellent enantio- and diastereoselectivity. High rotational energy barriers and configurational stability of the synthesized C–O atropisomers were identified through experimental studies. Furthermore, mechanistic investigations were conducted for gaining deep insights into this protocol. The synthetic utility was demonstrated through gram-scale synthesis and divergent transformations. This work provides a new synthetic paradigm for constructing C–O axially chiral architectures, and illuminates a promising perspective in the field of transition-metal-catalyzed C–H activation for the atroposelective construction of novel axial chirality.

Author contributions

Y. D., D. Y., and J.-L. N. conceived the concept and prepared the manuscript. Y. Z., Y. X., and B. G. conducted the experiments and analyzed the data. Y. Z. and Y. X. contributed equally to this work. All the authors participated in the discussions of the manuscript.

Conflicts of interest

There are no conflicts to declare.

Data availability

CCDC 2516693 (for **3za**) and 2504636 (for **5a**) contain the supplementary crystallographic data for this paper.[102a,b]

The data supporting this article have been included as part of the supplementary information (SI). Supplementary information: experimental procedures, optimization studies, mechanistic studies, and characterization data of new compounds. See DOI: https://doi.org/10.1039/d6sc02299e.

Acknowledgements

This work was supported by the Natural Science Foundation of Henan Province (242300421033, 252300421178, 232301420007, 242301420059), and National Natural Science Foundation of China (22271260, 22401266).

Notes and references

1 J. Yang, Z.-Y. Xie, Y.-J. Ye, S.-B. Ye, Y.-B. Wang, W.-T. Wang, P.-C. Qian, R.-J. Song, Q. Sun, L.-W. Ye and L. Li, *Sci. Adv.*, 2023, **9**, eadk1704.
2 Y.-F. Jiang, S. Tong, J. Zhu and M.-X. Wang, *Chem. Sci.*, 2024, **15**, 12517–12522.
3 Z.-Y. Zhang, T. Zhang, Y. Ouyang, P. Lu, J. X. Qiao and J.-Q. Yu, *Chem. Sci.*, 2024, **15**, 17092–17096.
4 F. Wang, W. Xiang, Y. Xie, L. Huai, L. Zhang and X. Zhang, *Sci. Adv.*, 2024, **10**, eadq2768.
5 A. Chu, B. Zhu, X. Zhang, H. Zhu, J. Zhang and X. Liu, *Sci. Adv.*, 2024, **10**, eadr1628.
6 F.-R. Huang, P. Zhang, Q.-J. Yao and B.-F. Shi, *CCS Chem.*, 2024, **6**, 2783–2793.
7 Y. Zhang, Y.-Z. Gu, K. Lu, Y.-P. Wang, A.-F. Wang, S.-H. Wang, S.-Q. Wei, F.-M. Zhang, X.-M. Zhang, A.-J. Ma, J.-B. Peng and Y.-Q. Tu, *CCS Chem.*, 2025, **7**, 1067–1077.
8 M. Koner, N. Ballav, A. J. Varma, S. Ghosh, T. Mondal, R. Kuniyil and M. Baidya, *Chem. Sci.*, 2025, **16**, 19296–19303.
9 Y. Ren, C. Lin, H. Zhang, Z. Liu, D. Wei, J. Feng and D. Du, *Chem. Sci.*, 2025, **16**, 7876–7883.
10 Y.-F. Zhang, B. Wang, Z. Chen, J.-R. Liu, N.-Y. Yang, J.-M. Xiang, J. Liu, Q.-S. Gu, X. Hong and X.-Y. Liu, *Science*, 2025, **388**, 283–291.
11 T. A. Schmidt, V. Hutskalova and C. Sparr, *Nat. Rev. Chem.*, 2024, **8**, 497–517.
12 A. Naghim, J. Rodriguez, O. Chuzel, G. Chouraqui and D. Bonne, *Angew. Chem., Int. Ed.*, 2024, **63**, e202407767.
13 N. Kotwal and P. Chauhan, *Chem. Commun.*, 2024, **60**, 6837–6846.
14 G.-J. Mei, W. L. Koay, C.-Y. Guan and Y. Lu, *Chem*, 2022, **8**, 1855–1893.
15 E. Kumarasamy, R. Raghunathan, M. P. Sibi and J. Sivaguru, *Chem. Rev.*, 2015, **115**, 11239–11300.
16 B. M. Duggan and D. J. Craik, *J. Med. Chem.*, 1997, **40**, 2259–2265.
17 K. C. Nicolaou, C. N. C. Boddy, S. Bräse and N. Winssinger, *Angew. Chem., Int. Ed.*, 1999, **38**, 2096–2152.

18 L. Ciasullo, A. Casapullo, A. Cutignano, G. Bifulco, C. Debitus, J. Hooper, L. Gomez-Paloma and R. Riccio, *J. Nat. Prod.*, 2002, **65**, 407–410.
19 B. M. Crowley and D. L. Boger, *J. Am. Chem. Soc.*, 2006, **128**, 2885–2892.
20 D. G. Brown and H. J. Wobst, *J. Med. Chem.*, 2021, **64**, 2312–2338.
21 R. D. Kavthe, J. R. A. Kincaid and B. H. Lipshutz, *ACS Sustainable Chem. Eng.*, 2022, **10**, 16896–16902.
22 F. Zhao, H. Zhang, M. Xie, B. Meng, N. Liu, C. Dun, Y. Qin, S. Gao, E. De Clercq, C. Pannecouque, Y.-J. Tang, P. Zhan, X. Liu and D. Kang, *J. Med. Chem.*, 2023, **66**, 2102–2115.
23 P. Msaouel, K. Yu, Y. Yuan, J. Chen, X. Yan, M. Karki, F. Duan, R. A. Sheth, P. Rao, K. Sircar, A. Y. Shah, A. J. Zurita, G. Genovese, M. Li, C.-C. Yeh, M. Dang, G. Han, Y. Chu, M. Hallin, P. Olson, R. Yang, D. Slavin, H. Der-Torossian, C. D. Chin, N. M. Tannir, L. Wang and J. Gao, *Nat. Commun.*, 2025, **16**, 578.
24 Y. Sato, M. Abekura, T. Oriki, Y. Nagashima, H. Uekusa and K. Tanaka, *Angew. Chem., Int. Ed.*, 2023, **62**, e202304041.
25 G. M. Adams and A. S. Weller, *Coord. Chem. Rev.*, 2018, **355**, 150–172.
26 M. Mohankumar, M. Holler, E. Meichsner, J.-F. Nierengarten, F. Niess, J.-P. Sauvage, B. Delavaux-Nicot, E. Leoni, F. Monti, J. M. Malicka, M. Cocchi, E. Bandini and N. Armaroli, *J. Am. Chem. Soc.*, 2018, **140**, 2336–2347.
27 S. Cen, N. Huang, D. Lian, A. Shen, M.-X. Zhao and Z. Zhang, *Nat. Commun.*, 2022, **13**, 4735.
28 R. Wang, Y. Wu, J. Wang, H. Huang, Y. Wang, S. Xu and F. Zhao, *J. Mol. Struct.*, 2022, **1257**, 132642.
29 M. S. Betson, J. Clayden, C. P. Worrall and S. Peace, *Angew. Chem., Int. Ed.*, 2006, **45**, 5803–5807.
30 K. Fuji, T. Oka, T. Kawabata and T. Kinoshita, *Tetrahedron Lett.*, 1998, **39**, 1373–1376.
31 R. Farooqi, A. Mustafai, A. G. Woldegiorgis, X. Lin and P. Wang, *ACS Catal.*, 2025, **15**, 7891–7911.
32 F. Hollmann, D. J. Opperman and C. E. Paul, *Angew. Chem., Int. Ed.*, 2021, **60**, 5644–5665.
33 J. Clayden, C. P. Worrall, W. J. Moran and M. Helliwell, *Angew. Chem., Int. Ed.*, 2008, **47**, 3234–3237.
34 B. Yuan, A. Page, C. P. Worrall, F. Escalettes, S. C. Willies, J. J. W. McDouall, N. J. Turner and J. Clayden, *Angew. Chem., Int. Ed.*, 2010, **49**, 7010–7013.
35 L. Dai, Y. Liu, Q. Xu, M. Wang, Q. Zhu, P. Yu, G. Zhong and X. Zeng, *Angew. Chem., Int. Ed.*, 2023, **62**, e202216534.
36 H. Bao, Y. Chen and X. Yang, *Angew. Chem., Int. Ed.*, 2023, **62**, e202300481.
37 J. Xu, W. Lin, H. Zheng and X. Li, *ACS Catal.*, 2024, **14**, 6667–6673.
38 S. Shee, S. Shree Ranganathappa, M. S. Gadhave, R. Gogoi and A. T. Biju, *Angew. Chem., Int. Ed.*, 2023, **62**, e202311709.
39 L. Li, W. Ti, T. Miao, J. Ma, A. Lin, Q. Chu and S. Gao, *J. Org. Chem.*, 2024, **89**, 4067–4073.
40 Y. Liu, L. Yuan, L. Dai, Q. Zhu, G. Zhong and X. Zeng, *J. Org. Chem.*, 2024, **89**, 7630–7643.
41 Y. Wu, X. Guan, H. Zhao, M. Li, T. Liang, J. Sun, G. Zheng and Q. Zhang, *Chem. Sci.*, 2024, **15**, 4564–4570.
42 B.-A. Zhou, X.-N. Li, C.-L. Zhang, Z.-X. Wang and S. Ye, *Angew. Chem., Int. Ed.*, 2024, **63**, e202314228.
43 A. Naghim, P. Solai, M. Giorgi, J.-V. Naubron, S. Humbel, R. Gupta, J. Rodriguez, O. Chuzel, G. Chouraqui and D. Bonne, *ChemistryEurope*, 2026, **4**, e70257.
44 L. Dai, X. Zhou, J. Guo, Q. Huang and Y. Lu, *Chem. Sci.*, 2024, **15**, 5993–6001.
45 X. Han, L. Chen, Y. Yan, Y. Zhao, A. Lin, S. Gao and H. Yao, *ACS Catal.*, 2024, **14**, 3475–3481.
46 Y. Wang, R. Mi, S. Yu and X. Li, *ACS Catal.*, 2024, **14**, 4638–4647.
47 Y. Li, S. Liu, B. Yuan, N. Graw and L. Ackermann, *Nat. Commun.*, 2026, **17**, 743.
48 Z. Han, L. Wei, C. Nian, X. Hu, S. Liu, H. Huang and J. Sun, *Sci. China Chem.*, 2026, **69**, 1266–1272.
49 A. N. Dinh, R. R. Noorbehesht, S. T. Toenjes, A. C. Jackson, M. A. Saputra, S. M. Maddox and J. L. Gustafson, *Synlett*, 2018, **29**, 2155–2160.
50 J. Wencel-Delord, A. Panossian, F. R. Leroux and F. Colobert, *Chem. Soc. Rev.*, 2015, **44**, 3418–3430.
51 G. Liao, T. Zhou, Q.-J. Yao and B.-F. Shi, *Chem. Commun.*, 2019, **55**, 8514–8523.
52 C.-X. Liu, W.-W. Zhang, S.-Y. Yin, Q. Gu and S.-L. You, *J. Am. Chem. Soc.*, 2021, **143**, 14025–14040.
53 G. Liao and B.-F. Shi, *Acc. Chem. Res.*, 2025, **58**, 1562–1579.
54 Q.-J. Yao and B.-F. Shi, *Acc. Chem. Res.*, 2025, **58**, 971–990.
55 T. Yang, Y. Zhang, Y. Dou, D. Yang and J.-L. Niu, *Sci. China Chem.*, 2026, **69**, 659–679.
56 F.-R. Huang, M.-Y. Teng, H. Qiu, Q.-J. Yao and B.-F. Shi, *Angew. Chem., Int. Ed.*, 2025, **64**, e202506465.
57 S. Fukagawa, Y. Kato, R. Tanaka, M. Kojima, T. Yoshino and S. Matsunaga, *Angew. Chem., Int. Ed.*, 2019, **58**, 1153–1157.
58 K. Ozols, S. Onodera, Ł. Woźniak and N. Cramer, *Angew. Chem., Int. Ed.*, 2021, **60**, 655–659.
59 Q.-J. Yao, J.-H. Chen, H. Song, F.-R. Huang and B.-F. Shi, *Angew. Chem., Int. Ed.*, 2022, **61**, e202202892.
60 X.-J. Si, D. Yang, M.-C. Sun, D. Wei, M.-P. Song and J.-L. Niu, *Nat. Synth.*, 2022, **1**, 709–718.
61 Y. Zhang, C. Yang, X. Meng, M. Wu, D. Yang, M.-P. Song and J.-L. Niu, *Org. Lett.*, 2025, **27**, 6076–6081.
62 Y. Zhang, S.-L. Liu, T. Li, M. Xu, Q. Wang, D. Yang, M.-P. Song and J.-L. Niu, *ACS Catal.*, 2024, **14**, 1–9.
63 T. Li, Y. Zhang, C. Du, D. Yang, M.-P. Song and J.-L. Niu, *Nat. Commun.*, 2024, **15**, 7673.
64 Y. Sun, T. Yang, Q. Wang, L. Shi, M.-P. Song and J.-L. Niu, *Org. Lett.*, 2024, **26**, 5063–5068.
65 T. Li, L. Shi, X. Zhao, J. Wang, X.-J. Si, D. Yang, M.-P. Song and J.-L. Niu, *Org. Lett.*, 2023, **25**, 5191–5196.
66 T. Li, L. Shi, X. Wang, C. Yang, D. Yang, M.-P. Song and J.-L. Niu, *Nat. Commun.*, 2023, **14**, 5271.
67 X.-J. Si, X. Zhao, J. Wang, X. Wang, Y. Zhang, D. Yang, M.-P. Song and J.-L. Niu, *Chem. Sci.*, 2023, **14**, 7291–7303.
68 X. Wang, X.-J. Si, Y. Sun, Z. Wei, M. Xu, D. Yang, L. Shi, M.-P. Song and J.-L. Niu, *Org. Lett.*, 2023, **25**, 6240–6245.

69 P.-F. Qian, Y.-X. Wu, J.-H. Hu, J.-H. Chen, T. Zhou, Q.-J. Yao, Z.-H. Zhang, B.-J. Wang and B.-F. Shi, *J. Am. Chem. Soc.*, 2025, **147**, 10791–10802.
70 P.-F. Qian, G. Zhou, J.-H. Hu, B.-J. Wang, A.-L. Jiang, T. Zhou, W.-K. Yuan, Q.-J. Yao, J.-H. Chen, K.-X. Kong and B.-F. Shi, *Angew. Chem., Int. Ed.*, 2024, **63**, e202412459.
71 Y.-J. Wu, Z.-K. Wang, Z.-S. Jia, J.-H. Chen, F.-R. Huang, B.-B. Zhan, Q.-J. Yao and B.-F. Shi, *Angew. Chem., Int. Ed.*, 2023, **62**, e202310004.
72 B.-J. Wang, G.-X. Xu, Z.-W. Huang, X. Wu, X. Hong, Q.-J. Yao and B.-F. Shi, *Angew. Chem., Int. Ed.*, 2022, **61**, e202208912.
73 X. Wu, Q. Tian, J. Ge, Y. Liu, Z. Li, J. Zhang and G. Cheng, *Chin. J. Chem.*, 2025, **43**, 2669–2676.
74 A. Das, S. Kumaran, P. Maity, J. R. Premkumar and B. Sundararaju, *J. Am. Chem. Soc.*, 2025, **147**, 26226–26237.
75 M. Tang and X. Yang, *Chem Catal.*, 2023, **3**, 100754.
76 P. Boos, N. K. Pandit, S. Dana, T. von Münchow, A. Hashidoko, L. Haberstock, R. Herbst-Irmer, D. Stalke and L. Ackermann, *ChemistryEurope*, 2025, **3**, e202500071.
77 A. Luc, J. C. A. Oliveira, P. Boos, N. Jacob, L. Ackermann and J. Wencel-Delord, *Chem Catal.*, 2023, **3**, 100765.
78 Y. Xu, Y. Lin, S. L. Homölle, J. C. A. Oliveira and L. Ackermann, *J. Am. Chem. Soc.*, 2024, **146**, 24105–24113.
79 T. von Münchow, Y.-R. Liu, R. Parmar, S. E. Peters, S. Trienes and L. Ackermann, *Angew. Chem., Int. Ed.*, 2024, **63**, e202405423.
80 S. Zhou, M. Wang, L. Wang, K. Chen, J. Wang, C. Song and J. Zhu, *Org. Lett.*, 2016, **18**, 5632–5635.
81 A. Dey and C. M. R. Volla, *Org. Lett.*, 2020, **22**, 7480–7485.
82 S. Zhai, S. Qiu, X. Chen, J. Wu, H. Zhao, C. Tao, Y. Li, B. Cheng, H. Wang and H. Zhai, *Chem. Commun.*, 2018, **54**, 98–101.
83 R. Mei, N. Sauermann, J. C. A. Oliveira and L. Ackermann, *J. Am. Chem. Soc.*, 2018, **140**, 7913–7921.
84 B. Schramm, M. Gray and J. M. Herbert, *J. Am. Chem. Soc.*, 2025, **147**, 3243–3260.
85 H.-H. Zhang, T.-Z. Li, S.-J. Liu and F. Shi, *Angew. Chem., Int. Ed.*, 2024, **63**, e202311053.
86 S.-C. Zhang, S. Liu, X. Wang, S.-J. Wang, H. Yang, L. Li, B. Yang, M. W. Wong, Y. Zhao and S. Lu, *ACS Catal.*, 2023, **13**, 2565–2575.
87 Y. Wang, X. Zhu, D. Pan, J. Jing, F. Wang, R. Mi, G. Huang and X. Li, *Nat. Commun.*, 2023, **14**, 4661.
88 S. Zhang, X. Wang, L.-L. Han, J. Li, Z. Liang, D. Wei and D. Du, *Angew. Chem., Int. Ed.*, 2022, **61**, e202212005.
89 S. Huang, H. Wen, Y. Tian, P. Wang, W. Qin and H. Yan, *Angew. Chem., Int. Ed.*, 2021, **60**, 21486–21493.
90 Q. Gao, C. Wu, S. Deng, L. Li, Z.-S. Liu, Y. Hua, J. Ye, C. Liu, H.-G. Cheng, H. Cong, Y. Jiao and Q. Zhou, *J. Am. Chem. Soc.*, 2021, **143**, 7253–7260.
91 T. A. Schmidt and C. Sparr, *Acc. Chem. Res.*, 2021, **54**, 2764–2774.
92 O. M. Beleh, E. Miller, F. D. Toste and S. J. Miller, *J. Am. Chem. Soc.*, 2020, **142**, 16461–16470.
93 X. Bao, J. Rodriguez and D. Bonne, *Chem. Sci.*, 2020, **11**, 403–408.
94 X. Bao, J. Rodriguez and D. Bonne, *Angew. Chem., Int. Ed.*, 2020, **59**, 12623–12634.
95 W. Xia, Q.-J. An, S.-H. Xiang, S. Li, Y.-B. Wang and B. Tan, *Angew. Chem., Int. Ed.*, 2020, **59**, 6775–6779.
96 Y.-L. Hu, Z. Wang, H. Yang, J. Chen, Z.-B. Wu, Y. Lei and L. Zhou, *Chem. Sci.*, 2019, **10**, 6777–6784.
97 Q. Dherbassy, J.-P. Djukic, J. Wencel-Delord and F. Colobert, *Angew. Chem., Int. Ed.*, 2018, **57**, 4668–4672.
98 Y. Yang, C. Yang, X. Zhang, Y. Tian, X. Cheng, T. Zeng and B. Li, *ACS Catal.*, 2025, **15**, 3442–3450.
99 N.-Y. Wang, S. Gao, Z.-D. Shu, B.-B. Cheng, C. Ma, Y.-C. Zhang and F. Shi, *Sci. China Chem.*, 2025, **68**, 3130–3137.
100 W. Zhang, S. Chen, Y. Zhang, S. Liu and X. Shen, *Angew. Chem., Int. Ed.*, 2025, **64**, e202422020.
101 A. Lerchen, S. Vásquez-Céspedes and F. Glorius, *Angew. Chem., Int. Ed.*, 2016, **55**, 3208–3211.
102 (*a*) CCDC 2516693: Experimental Crystal Structure Determination, 2025, DOI: 10.5517/ccdc.csd.cc2qgtnp; (*b*) CCDC 2504636: Experimental Crystal Structure Determination, 2025, DOI: 10.5517/ccdc.csd.cc2q28qt.